Secondary Structure and Orientation of Phospholamban Reconstituted in Supported Bilayers from Polarized Attenuated Total Reflection FTIR Spectroscopy†

Suren A. Tatulian,*,‡ Larry R. Jones,§ Laxma G. Reddy,‡ David L. Stokes,‡ and Lukas K. Tamm*,‡

Department of Molecular Physiology and Biological Physics, University of Virginia, Health Sciences Center, Box 449, Charlottesville, Virginia 22908, and Krannert Institute of Cardiology, Department of Medicine, Indiana University School of Medicine, Indianapolis, Indiana 46202

Received September 1, 1994; Revised Manuscript Received January 25, 1995⊗

ABSTRACT: We have studied the secondary structure of native phospholamban (PLB), a 52-residue integral membrane protein that regulates calcium uptake into the cardiac sarcoplasmic reticulum, as well as its 27-residue carboxy-terminal transmembrane segment (PLB_{26-52}). The relative contents of α-helix, β-strand, and random coil, as well as the spatial orientations of the α-helices of these molecules, reconstituted in dimyristoylphosphatidylcholine (DMPC) and 1-palmitoyl-2-oleoylphosphatidylcholine (POPC) bilayer membranes, were determined using polarized attenuated total reflection (ATR) Fourier transform infrared (FTIR) spectroscopy. The major component of the amide I′ bands of PLB and PLB_{26-52} was centered at 1654−1657 cm^{-1} and was assigned to α-helix. The fraction of α-helix in native PLB was 64−67% (33−35 residues), and the transmembrane peptide PLB_{26-52} contained 73−82% α-helix (20−22 residues); small fractions of β- and random structures were also identified. The orientational order parameter (S) of the α-helical component of PLB_{26-52} in DMPC was $S = 0.86 \pm 0.09$, indicating that the transmembrane helix was oriented approximately perpendicular to the membrane plane. Assuming the transmembrane domain of PLB resembles the peptide PLB_{26-52}, the additional α-helical residues in PLB were assigned to the cytoplasmic helix and determined to have an order parameter $S = -0.15 \pm 0.30$. This may imply that the cytoplasmic helix was tilted from the membrane normal by an angle of 61 ± 13° or, alternatively, may indicate a wide angular distribution. PLB reconstituted in the supported DMPC bilayers was phosphorylated by the catalytic subunit of protein kinase A, as confirmed by the appearance of a new absorbance band at ~1200 cm^{-1}. Phosphorylation reduced the α-helical content of PLB to 54% (~28 residues), though the orientation of the cytoplasmic helix was not significantly changed. These results, in conjunction with Chou−Fasman secondary structure prediction, are consistent with a model of PLB composed of a transmembrane helix (residues 33−52), a cytoplasmic helix (most likely residues 8−20), and a small intervening β-sheet between residues 22 and 32 as well as a random coil at the amino terminus of the protein.

Phospholamban (PLB)[1] is a 52-residue integral membrane protein localized to cardiac muscle which regulates the activity of the sarcoplasmic reticulum (SR) Ca^{2+}-ATPase (Tada & Kadoma, 1989). In its dephosphorylated state PLB inhibits the Ca^{2+}-ATPase; phosphorylation of PLB either by cAMP-dependent or by Ca^{2+}−calmodulin-dependent protein kinase restores full activity to the enzyme (Le Peuch et al., 1979; Tada & Kadoma, 1989). By this mechanism PLB mediates increased contractility of heart muscle in response to β-adrenergic stimulation (Lindemann et al., 1983; Sham et al., 1991). PLB is also expressed in the SR of slow-twitch skeletal muscle (Jorgensen & Jones, 1986; Fujii et al., 1988; Szimanska et al., 1991; Briggs et al., 1992), though at lower levels, and in this case its physiological effect is less clear.

The primary structure of PLB deduced from amino acid (Simmerman et al., 1986) and cDNA (Fujii et al., 1987) sequence analysis is presented in Figure 1. Two major domains of the protein have been identified: a hydrophilic, cytoplasmic domain (domain I, residues 1−30) and a hydrophobic, membrane-spanning domain (domain II, residues 31−52) (Wegener et al., 1986; Simmerman et al., 1986; Tada & Kadoma, 1989). Domain I has three excess positive charges that line up on one face when projected in helical wheel format, leading to a suggestion for an amphipathic helix between residues 7 and 17 (Morris et al., 1991). The two sites of phosphorylation, Ser-16 and Thr-17, are found in this domain (Simmerman et al., 1986; Wegener et al., 1986). The transmembrane domains associate to form noncovalent homopentamers in sodium dodecyl sulfate (SDS) gels (Wegener & Jones, 1984; Simmerman et al., 1986; Arkin

† This work was supported by Grant VA-93-F16 from the American Heart Association, Virginia Affiliate, to S.A.T. and by grants from the NIH to L.R.J., D.L.S., and L.K.T.

‡ University of Virginia Health Sciences Center.

§ Indiana University School of Medicine.

⊗ Abstract published in *Advance ACS Abstracts,* March 15, 1995.

[1] Abbreviations: ATP, adenosine triphosphate; ATR, attenuated total reflection; βOG, octyl β-glucoside; cAMP, cyclic adenosine monophosphate; CD, circular dichroism; $C_{12}E_8$, *n*-dodecyloctaethylene glycol monoether; DMPC, dimyristoylphosphatidylcholine; DTT, dithiothreitol; EGTA, ethylene glycol bis(β-aminoethyl ether)-*N*,*N*,*N*′,*N*′-tetraacetic acid; FTIR, Fourier transform infrared; IR, infrared; MOPS, morpholinopropanesulfonic acid; NMR, nuclear magnetic resonance; PAGE, polyacrylamide gel electrophoresis; PBS, phosphate buffered saline (10 mM sodium phosphate + 150 mM sodium chloride, pH 7.2); PKA, protein kinase A (cAMP-dependent protein kinase); PLB, phospholamban; PLB_{26-52}, carboxy-terminal 27-residue peptide of phospholamban (residues 26−52); PMSF, phenylmethanesulfonyl fluoride; POPC, 1-palmitoyl-2-oleoylphosphatidylcholine; P-PLB, phosphorylated phospholamban; SDS, sodium dodecyl sulfate; SR, sarcoplasmic reticulum; TES, *N*-tris(hydroxymethyl)methyl-2-aminomethanesulfonic acid; TFE, trifluoroethanol; TPCK, *N*-tosyl-L-phenylalanyl chloromethyl ketone; Tris, tris(hydroxymethyl)aminomethane.

0006-2960/95/0434-4448$09.00/0

		(-)	(+)						(+)				(+)	(+)				
	Ac·Met$_1$	Asp	Lys	Val	Gln$_5$	Tyr	Leu	Thr	Arg	Ser$_{10}$	Ala	Ile	Arg	Arg	Ala$_{15}$	Ser	Thr	Ile
Chou-Fasman	•	•	•	B	B	B	B	B	h	h	h	h	h	h	h	h	h	h
Our assignment	r	r	r	r	r	r	r	H	H	H	H	H	H	H	H	H	H	H

	(-)						(+)										
	Glu	Met$_{20}$	Pro	Gln	Gln	Ala	Arg$_{25}$	Gln	Asn	Leu	Gln	Asn$_{30}$	**Leu**	**Phe**	**Ile**	**Asn**	**Phe$_{35}$**
Chou-Fasman	h	h	•	b	b	b	b	b	b	b	b	b	b	b			
Our assignment	H	H	•	•	B	B	B	t	t	t	t	B	B	B	H	H	H

	Cys	**Leu**	**Ile**	**Leu**	**Ile$_{40}$**	**Cys**	**Leu**	**Leu**	**Leu**	**Ile$_{45}$**	**Cys**	**Ile**	**Ile**	**Val**	**Met$_{50}$**	**Leu**	**Leu**
Our assignment	H	H	H	H	H	H	H	H	H	H	H	H	H	H	H	H	H

FIGURE 1: Primary structure of phospholamban, accompanied with our assignment of the secondary structure (see text). A secondary structure prediction of the cytoplasmic domain I (residues 1−30) according to Chou−Fasman is also shown. The hydrophobic transmembrane domain II (residues 31−52) is outlined in bold. The letters B, b, H, h, r, and t refer to strong β, β, strong α, α, random, and turn, respectively. The dots refer to random structure or indifference toward any secondary structure. Charges of ionized residues are shown in parentheses.

et al., 1994). Direct evidence for the oligomeric state of PLB in SR membranes or lipid bilayers has not been presented to date.

PLB could alter active Ca^{2+} sequestration in cardiac SR by at least four different mechanisms. First, a wide variety of evidence, including chemical crosslinking and site-directed mutagenesis, suggests that PLB interacts directly with Ca^{2+}-ATPase and thereby inhibits the enzyme (Tada & Kadoma, 1989; James et al., 1989; Toyofuku et al., 1993, 1994). Second, neutralization (pI = 6.7) of the highly basic (pI = 11.0) PLB upon phosphorylation (Jones et al., 1985) may increase the apparent affinity of Ca^{2+}-ATPase for Ca^{2+} by increasing the local concentration of Ca^{2+} at the membrane surface (Chiesi & Schwaller, 1989). Third, pentameric PLB may itself form a Ca^{2+}-selective channel and thereby regulate Ca^{2+} pumping (Simmerman et al., 1986; Kovacs et al., 1988; Arkin et al., 1993, 1994). Finally, time-resolved phosphorescence anisotropy experiments suggested that unphosphorylated PLB may mediate aggregation of Ca^{2+}-ATPase monomers (Voss et al., 1994) and thus slow the rate-limiting step of the enzyme reaction cycle (Cantilina et al., 1993).

In order to better understand the molecular mechanism of regulation of the Ca^{2+}-ATPase by PLB, more detailed information on the structure of both proteins is required. However, little is known concerning the structure of PLB in membranes. Circular dichroism (CD) spectroscopy was utilized to determine the secondary structure of PLB and its fragments solubilized in detergent micelles (Simmerman et al., 1989; Vorherr et al., 1993) or dissolved in a mixture of trifluoroethanol (TFE) and aqueous buffer (Terzi et al., 1992). Preliminary NMR data have recently been reported on the secondary structure of PLB_{1-25} (Mortishire-Smith et al., 1994). In all cases PLB proved to be highly (68−80%) α-helical and phosphorylation had little effect on helical content (see Table 2). However, in none of the previous studies was PLB reconstituted in its natural environment, i.e., a lipid bilayer. Furthermore, although it was speculated that the regulatory effects of PLB on Ca^{2+}-ATPase might be due to a reorientation of domain I with respect to domain II upon phosphorylation (Tada & Kadoma, 1989; Simmerman et al., 1989), no attempts have been undertaken to determine the spatial orientation of the cytoplasmic and transmembrane domains of PLB.

We have used polarized attenuated total reflection (ATR) Fourier transform infrared (FTIR) spectroscopy to investigate the secondary structure and orientation of PLB reconstituted in substrate-supported phospholipid bilayers and to study the effect of phosphorylation on the structure of PLB *in situ*. On the basis of these measurements and on secondary structure prediction, we present a structural model for PLB in lipid membranes.

THEORY

The orientation of a structural element of a molecule can be determined by polarized ATR infrared (IR) spectroscopy from the dichroic ratio:

$$R^{\mathrm{ATR}} = \frac{A_{\parallel}}{A_{\perp}} = \frac{\int A_{\parallel}(\nu)\, d\nu}{\int A_{\perp}(\nu)\, d\nu} \qquad (1)$$

where $A_{\parallel}$ and $A_{\perp}$ are the integrated absorbances of a given band and $A_{\parallel}(\nu)$ and $A_{\perp}(\nu)$ are the absorbances at frequency ν for the polarizations of the IR beam parallel and perpendicular to the incidence plane, respectively. For a liquid-crystalline lipid bilayer, supported on an internal reflection plate parallel to the *XY* plane and excited by the evanescent field of an internally reflected IR beam, which is incident in a plane parallel to the *Z* axis, the ATR dichroic ratio becomes (Fringeli, 1992)

$$R^{\mathrm{ATR}} = \frac{E_x^2}{E_y^2} + \frac{E_z^2[1 + S(3\cos^2\alpha - 1)]}{E_y^2[1 - 0.5S(3\cos^2\alpha - 1)]} \qquad (2)$$

where

$$E_x = \frac{2\cos\gamma\sqrt{\sin^2\gamma - n_{31}^2}}{\sqrt{(1 - n_{31}^2)[(1 + n_{31}^2)\sin^2\gamma - n_{31}^2]}}$$

$$E_y = \frac{2\cos\gamma}{\sqrt{1 - n_{31}^2}}$$

$$E_z = \frac{n_{32}^2 \sin 2\gamma}{\sqrt{(1 - n_{31}^2)[(1 + n_{31}^2)\sin^2\gamma - n_{31}^2]}}$$

are the components of the electric vector of the evanescent wave at the solid−liquid interface (Harrick, 1979), $n_{ij} \equiv n_i/n_j$, n_1, n_2, and n_3 are the refractive indices of the internal

reflection plate, of the supported bilayer, and of the bathing aqueous phase, respectively, α is the angle between the transition dipole moment and the main axis of symmetry (molecular director) of the structural element under consideration, e.g., the long axis of a helix, γ is the angle of incidence of the IR beam, S is the order parameter and is a time- and space-averaged function of the angle θ between the molecular director and the Z axis:

$$S = (3\langle\cos^2\theta\rangle - 1)/2 \quad (3)$$

Equation 2 is only correct for distributions that are axially symmetric around Z. It is generally assumed that all molecules exhibit an axially symmetric distribution in a liquid-crystalline bilayer. An expression for S can be obtained by rearranging eq 2:

$$S = \frac{2(E_x^2 - R^{ATR}E_y^2 + E_z^2)}{(3\cos^2\alpha - 1)(E_x^2 - R^{ATR}E_y^2 - 2E_z^2)} \quad (4)$$

i.e., the equation that we have previously used to determine the orientation of single α-helices in supported lipid bilayers (Frey & Tamm, 1991; Tamm & Tatulian, 1993).

This concept, which has been derived for a single structural element (or for several structural elements with similar orientation), may now be extended to a system with several such elements that are detected by the same absorption band but may have different orientational distributions. In this case, the total dichroic ratio is simply the ratio of the sums of the parallel and perpendicular absorbances of the individual component elements (Fringeli, 1992):

$$R_T^{ATR} = \frac{\sum x_i[E_x^2(1 - 0.5\sigma_i) + E_z^2(1 + \sigma_i)]}{E_y^2\sum x_i(1 - 0.5\sigma_i)} \quad (5)$$

where x_i is the mole fraction of the ith component and $\sigma_i = S_i(3\cos^2\alpha - 1)$.

In this work, we consider a molecule with two α-helices that may have different orientational distributions. If the angle between these two helices is not known, then the order parameters S_1 and S_2 cannot be determined from the measurement of a single dichroic ratio. However, if S_1 is determined in an independent experiment, S_2 can be deduced from the measurement of R_T^{ATR} using eq 5:

$$S_2 = \{x_1[(E_x^2 - R_T^{ATR}E_y^2)(1 - 0.5\sigma_1) + E_z^2(1 + \sigma_1)] + x_2(E_x^2 + E_z^2 - R_T^{ATR}E_y^2)\}/\{x_2(3\cos^2\alpha - 1)[0.5(E_x^2 - R_T^{ATR}E_y^2) - E_z^2]\} \quad (6)$$

As seen from eq 3, the limiting values of the order parameter are $S = -0.5$ and 1.0, which correspond to fixed orientations of the molecular director perpendicular and parallel to the Z axis, respectively.

MATERIALS AND METHODS

Materials. Recombinant PLB was expressed in Sf21 insect cells and purified by monoclonal antibody affinity chromatography as briefly described by Cala et al. (1993) and to be described in detail elsewhere (Reddy et al., 1995). The final concentration of PLB was ~1 mg/mL in 0.92% octyl β-glucoside (βOG), 18 mM glycine, 83 mM MOPS, and 5 mM DTT (pH 7.2). The purity of recombinant PLB was verified directly by protein sequencing (Simmerman et al., 1986). We found that the amino terminus of the recombinant protein was blocked, as is the case for canine cardiac PLB (Fujii et al., 1986). Treatment of recombinant PLB with endoproteinase Lys-C (Boehringer Mannheim) allowed the expected sequence to be determined, beginning with amino acid residue 4 (valine). This protease-treated PLB was sequenced through 25 consecutive residues, and no extraneous sequences were found. For generation of PLB_{26-52}, 776 μg of purified recombinant PLB in the buffer above was incubated for 24 h at room temperature with 78 μg of TPCK-treated trypsin (Sigma) in a final volume of 1.2 mL. The pH was adjusted to 7.8 by adding concentrated MOPS. After proteolysis, PMSF was added to a final concentration of 0.2 mM. The sample was then passed over 0.2 mL of CM Sepharose preequilibrated with 20 mM MOPS, 1% βOG, and 1 mM DTT. PLB_{26-52} was recovered in the flow-through fraction, whereas the trypsin was retained by the column. PLB_{26-52} was then concentrated and diluted three times consecutively with 20 mM MOPS, 1% βOG, and 1 mM DTT using a Centricon 30 filter (Amicon); thus, the smaller proteolytic fragments were separated from PLB_{26-52}. The final volume of purified PLB_{26-52} was 0.5 mL. The primary structure of PLB_{26-52} was verified by protein sequencing. The sequence began at Gln-26, and no extraneous sequence was detected through 26 consecutive residues. Figure 2 documents the purity of recombinant PLB and the derived peptide PLB_{26-52} by SDS−PAGE and demonstrates the ability of both species to form pentamers. Boiling either preparation in SDS prior to electrophoresis completely destabilized the pentameric mobility form (P), converting it mostly into monomers (M); consistent with previous results on native PLB, some intermediate mobility forms were also visible. Even with loading 10 μg of protein sample per gel lane, no contaminant bands were detected.

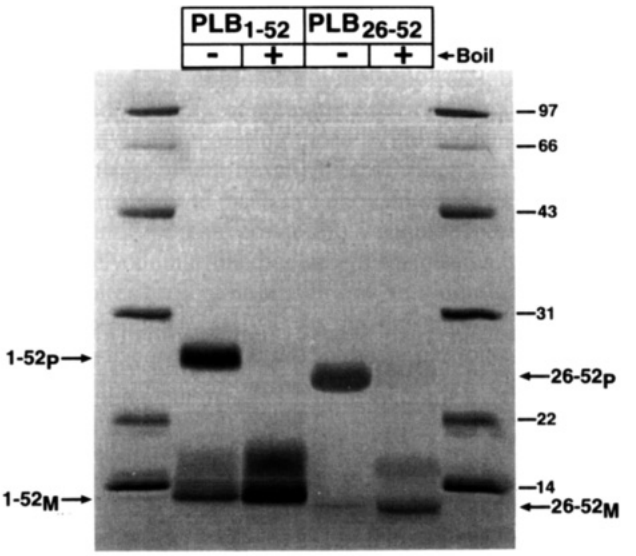

FIGURE 2: SDS−PAGE of recombinant PLB and of its tryptic fragment PLB_{26-52}. 10 μg of recombinant PLB and PLB_{26-52} were electrophoresed per gel lane as indicated. Shown is the Coomassie Blue stained gel. Samples contained 7.5% SDS, and "Boil" indicates samples that were placed in a boiling water bath for 3 min just prior to electrophoresis. The pentameric (P) and monomeric (M) mobility forms of PLB are indicated by the arrows. Some phospholamban dimers, trimers, and tetramers are also faintly visible. Molecular weight standards (in kilodaltons) are shown in the far right and left lanes.

Dimyristoylphosphatidylcholine (DMPC) and 1-palmitoyl-2-oleoylphosphatidylcholine (POPC) were purchased from Avanti Polar Lipids, Inc. (Alabaster, AL). All other chemicals were from Sigma Chemical Co. (St. Louis, MO), Fisher (Fair Lawn, NJ), or Eastman Kodak (Rochester, NY) and were of the highest available purity. Bio-Beads SM-2 were from Bio-Rad Laboratories (Richmond, CA).

Polyacrylamide Gel Electrophoresis and Protein Assay. Protein concentration was determined by the method of Schaffner and Weissmann (1973). SDS−PAGE was performed according to Laemmli (1970) using a 7−18% polyacrylamide with a 3% stacking gel. The gel was stained with Coomassie Blue.

Reconstitution of PLB and PLB_{26-52} in Lipid Vesicles. For the reconstitution of PLB in lipid vesicles, 10 mg of Bio-Beads was added to 100 μL of suspension containing 30 μg of PLB and 0.28 mg of βOG and stirred for 3 h at room temperature. Then the sample was separated from the Bio-Beads and lyophilized for 1 h. To the lyophilized PLB 90 μL of 5 mM phospholipid in chloroform was added. To improve the solubilization of the protein, 2−3 drops of TFE was added. The solvent was evaporated under a stream of nitrogen, 0.75 mL of PBS was added, and the suspension was vigorously vortexed for 4−5 min and was sonicated at 0−5 °C with a microtip sonifier for 30 s.

To reconstitute the hydrophobic peptide PLB_{26-52} in lipid vesicles, 800 nmol of DMPC or POPC in chloroform was dried under nitrogen, suspended in 0.3 mL of PBS, vortexed, and frozen and thawed five times using liquid nitrogen and hot water, followed by 15 cycles of extrusion through a pair of 100 nm pore size polycarbonate membranes (Nucleopore, Pleasanton, CA) using a syringe-type Liposofast extruder (Avestin, Ottawa, Canada). To incorporate PLB_{26-52} into these vesicles, 11−15 μg of PLB_{26-52} in 0.3−0.4 mg of βOG was added to the extruded vesicles, and βOG was removed by adding 10 mg of Bio-Beads and shaking for 3 h at room temperature. The sample was then separated from the Bio-Beads, extruded, and diluted to a final volume of 0.7 mL.

Reconstitution of PLB and PLB_{26-52} in Supported Bilayers. Planar phospholipid bilayers containing PLB or PLB_{26-52} were prepared by the monolayer fusion procedure described by Frey and Tamm (1991) and Tamm and Tatulian (1993). Briefly, a DMPC or POPC monolayer was transferred from a Langmuir trough filled with 10 mM Tris-acetic acid and 0.002% NaN_3 (pH 5.0) onto the surface of a clean germanium internal reflection plate (50 × 20 × 1 mm^3) at a constant surface pressure of 32 mN/m. The plate was then assembled in between two identical halves of the measuring cell. Approximately 0.7 mL of the proteoliposome suspension was injected into the cell and incubated at room temperature for 1.5−2 h to allow the vesicles to fuse with the monolayer and to yield supported lipid bilayers with reconstituted PLB or PLB_{26-52} on both surfaces of the germanium plate. The excess unfused vesicles were flushed with 7 mL of D_2O.

Phosphorylation of Phospholamban. PLB was phosphorylated by freshly prepared buffer containing 10 units/mL (0.2 mg/mL) of the catalytic subunit of PKA, 5 mM ATP, 10 mM $MgCl_2$, 0.5 mM EGTA, 0.3 M sucrose, and 50 mM MOPS (pH 7.0); 0.5 mL of this buffer was injected into the cell containing PLB reconstituted in supported bilayers and incubated at room temperature for 1 h. After the reaction medium was flushed with D_2O and the spectra were recorded, no changes in the areas of amide I′ bands were detected, implying that PKA did not tightly bind to the membranes and could easily be removed.

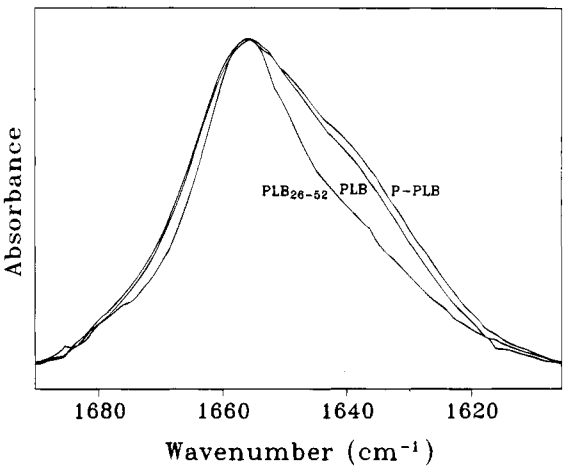

FIGURE 3: Amide I′ absorbance bands of PLB_{26-52}, PLB, and P-PLB reconstituted in DMPC bilayers supported on germanium plates in D_2O at parallel polarization of the IR beam.

Infrared Spectroscopy. Polarized infrared spectra were recorded on a Nicolet 740 FTIR spectrometer equipped with an ATR-FTIR accessory as previously described (Tamm & Tatulian, 1993). Typically, 2000 scans were collected at each polarization with a resolution of 2 cm^{-1}. ATR spectra of D_2O recorded under identical conditions were used as references. The instrument was purged with nitrogen to remove H_2O vapor. The absorbance of the residual H_2O vapor was subtracted to get a flat, featureless line between 2100 and 1800 cm^{-1}, where neither protein nor lipid absorb considerably (Arrondo et al., 1993).

Processing of Infrared Spectra. The ATR-FTIR spectra were processed using the Lab Calc software (Galactic Industries, Salem, NH). The baselines of amide I′ absorbance bands were corrected in the amide I′ region. To identify the positions of the component peaks of the amide I′ band, the spectra were differentiated two times, accompanied with 11-point Savitsky−Golay smoothing. The peak wavenumbers of the second derivative curves were used as starting parameters for curve-fitting. The results of the amide I′ band decompositions were regarded as satisfactory if (a) the difference between the starting and final wavenumbers of the individual peaks did not exceed 2 cm^{-1}, (b) all the component peaks had reasonable half-widths (<20−25 cm^{-1}), and (c) the difference between the original end fitted curves was sufficiently small ($\chi^2 < 5 \times 10^{-6}$). After identification of the individual components, the absolute areas of the peaks centered at ~1656 cm^{-1}, corresponding to α-helix (Byler & Susi, 1986; Arrondo et al., 1993), were used to evaluate the orientations of helices. The ratio of these areas at parallel and perpendicular polarizations yielded the ATR dichroic ratio (R^{ATR}). The order parameters and orientations of helices were calculated from R^{ATR} values as described under Theory.

RESULTS

The ATR-FTIR absorbance spectra of PLB_{26-52}, PLB, and P-PLB in the amide I′ region are shown in Figure 3. In all cases the peaks of the amide I′ bands are centered at 1654−1657 cm^{-1} indicating a large fraction of α-helix in all three

Table 1: Assignment, Wavenumbers (ν), and Relative Areas of the Component Peaks Deduced from the Decomposition of the Amide I′ Absorbance Bands of PLB_{26-52}, PLB, and P-PLB Reconstituted in DMPC Bilayers and of PLB_{26-52} and PLB Reconstituted in POPC Bilayers Supported on Germanium Substrate[a]

	PLB_{26-52}		PLB		P-PLB	
assignment	ν (cm^{-1})	relative area (%)	ν (cm^{-1})	relative area (%)	ν (cm^{-1})	relative area (%)
DMPC						
β-strand	1676 ± 2.8	4.2 ± 1.3	1677 ± 2.2	4.5 ± 1.0	1676 ± 2.7	5.3 ±1.4
α-helix	1656 ± 1.4	73.2 ± 3.4	1656 ± 1.8	64.4 ± 4.2	1656 ± 2.1	54.5 ± 3.3
random	1640 ± 2.7	13.4 ± 2.4	1638 ± 3.4	24.6 ± 1.9	1639 ± 1.7	33.6 ± 3.0
β-strand	1631 ± 2.5	8.8 ± 2.1	1629 ± 1.7	3.7 ± 0.8	1633 ± 2.6	<1
β-strand	1620 ± 1.6	<1	1623 ± 2.3	2.8 ± 0.6	1624 ± 1.8	6.3 ± 1.5
POPC						
β-strand	1674 ± 3.1	10.7 ± 2.9	1672 ± 2.4	2.7 ± 1.3		
α-helix	1657 ± 0.8	82.2 ± 4.6	1655 ± 2.2	66.8 ± 2.7		
random	1641 ± 2.7	6.2 ± 1.3	1639 ± 2.8	24.2 ± 3.2		
β-strand	1630 ± 2.2	<1	1629 ± 2.1	5.1 ± 2.6		
β-strand	1619 ± 2.3	<1	1620 ± 1.7	1.2 ± 0.8		

[a] All values are given as mean ± standard deviations.

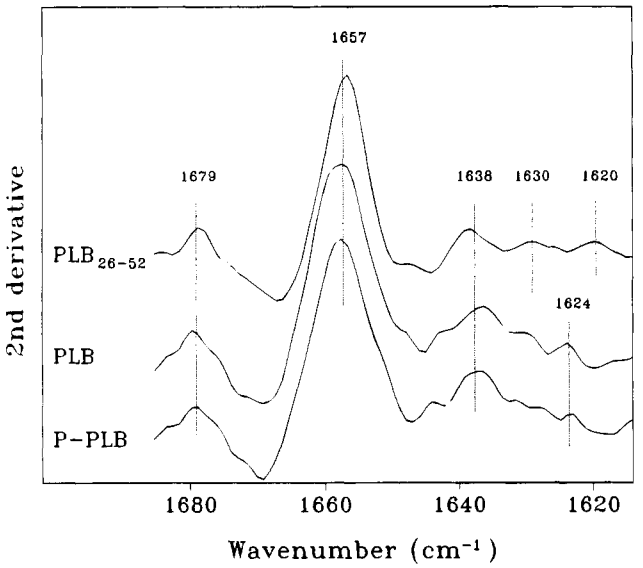

FIGURE 4: Second derivatives of the parallel polarized amide I′ spectra of PLB_{26-52}, PLB, and P-PLB reconstituted in DMPC bilayers. The dotted lines indicate the approximate peak positions of the second derivative curves, which correspond to the positions of the components of the amide I′ band. The spectra were inverted along the ordinate to facilitate the identification of the component peaks.

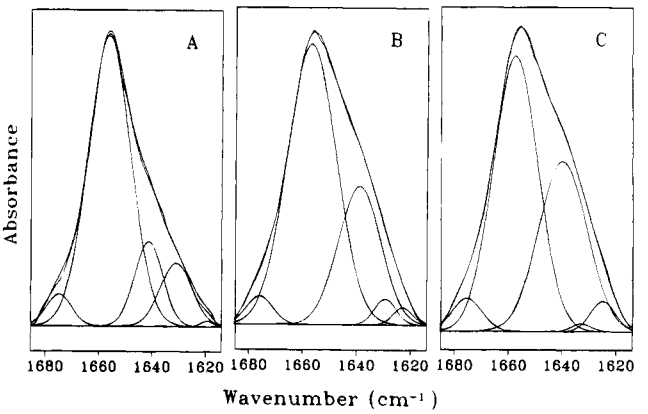

FIGURE 5: Spectral decomposition of the amide I′ bands of PLB_{26-52} (A), PLB (B), and P-PLB (C). The Gaussian component peaks are the result of curve-fitting using the frequencies of the components deduced from the second derivatives. The sums of the fitted components nearly superpose with the experimental amide I′ bands.

molecules. Despite the near superposition of peak wavenumbers of the three amide I′ bands, the shapes of these bands are distinctly different with a broad shoulder appearing at 1630−1640 cm^{-1} in the spectra of PLB and P-PLB. As will be shown in more detail below, this may be attributed to higher contents of β- and random structures in the full length molecule as compared to the transmembrane peptide.

To determine the relative contents of different secondary structures in these molecules, the amide I′ absorbance bands were decomposed by curve-fitting. The second derivatives of the amide I′ absorbance bands of PLB_{26-52}, PLB, and P-PLB, which were used to identify the frequencies of the components of the amide I′ bands, are shown in Figure 4. These curves demonstrate that the major component of the amide I′ bands in all three spectra is centered at ~1656 cm^{-1}, which is characteristic of α-helix (Byler & Susi, 1986; Mendelsohn & Mantsch, 1986; Krimm & Bandekar, 1986; Arrondo et al., 1993). The derivative curves also demonstrate weaker peaks at 1637−1640 cm^{-1}, typical for deuterated random coil, and at 1620−1630 and ~1679 cm^{-1}, which are assigned to antiparallel β-structure (Byler & Susi, 1986; Krimm & Bandekar, 1986; Mendelsohn & Mantsch, 1986; Arrondo et al., 1993). These wavenumbers were used as starting parameters for a curve-fitting program which refined the positions and relative contributions of the component peaks. The decomposed amide I′ bands of PLB_{26-52}, PLB, and P-PLB are presented in Figure 5. The agreement between the starting and resulting wavenumbers was better than 2 cm^{-1} (which is the spectral resolution of these measurements) for all components except the small peak at ~1677 cm^{-1}, for which the deviation was 2−4 cm^{-1}.

The quantitative results of the amide I′ band decompositions of PLB_{26-52}, PLB, and P-PLB reconstituted in DMPC and POPC bilayers are summarized in Table 1. In the case of DMPC, the relative area of the α-helical component is 73% for PLB_{26-52}, 64% for PLB, and 54% for P-PLB. Figure 5 and Table 1 also show significant fractions of random structure in PLB and P-PLB, represented by the component at 1638−1640 cm^{-1} (25% and 34%, respectively). The spectra exhibit three additional components at 1674−1677, 1629−1633, and 1620−1624 cm^{-1}, which are likely to represent the splitted amide I′ vibrational modes of an antiparallel β-sheet (Miyazawa, 1960; Krimm & Abe, 1972; Krimm & Bandekar, 1986; Surewicz et al., 1993). The numbers of residues in a particular secondary structure were determined from the relative component areas by assuming

Table 2: Secondary Structure of PLB, P-PLB, and Their Fragments under Different Conditions

molecule	conditions	method	content[f] α-helix	content[f] β-strand	content[f] random	reference
PLB	DMPC	FTIR	64% (33)	11% (6)	25% (13)	*a*
PLB	POPC	FTIR	67% (35)	9% (5)	24% (12)	*a*
PLB	2% SDS	CD	72% (37)	14% (7)	13% (7)	*b*
PLB	0.075% $C_{12}E_8$	CD	68% (35)	2% (1)	18% (9)	*c*
P-PLB	DMPC	FTIR	54% (28)	12% (6)	33% (17)	*a*
P-PLB	2% SDS	CD	69% (36)	14% (7)	16% (8)	*b*
PLB_{1-25}	30% TFE/H_2O	CD	60% (15)	N/R[g]	N/R	*d*
PLB_{1-25}	30% TFE/H_2O	NMR	68% (17)	N/R	32% (8)	*d*
P-PLB_{1-25}	30% TFE/H_2O	CD	25% (6)	N/R	N/R	*d*
P-PLB_{1-25}	30% TFE/H_2O	NMR	46% (12)	N/R	54% (13)	*d*
PLB_{2-33}	40% TFE/PBS	CD	33% (11)	N/R	N/R	*e*
P-PLB_{2-33}	40% TFE/PBS	CD	25% (8)	N/R	N/R	*e*
PLB_{26-52}	DMPC	FTIR	73% (20)	14% (4)	13% (4)	*a*
PLB_{26-52}	POPC	FTIR	82% (22)	6% (2)	12% (3)	*a*
PLB_{26-52}	2% SDS	CD	66% (18)	33% (9)	0% (0)	*b*

[a] This work. [b] Simmerman et al. (1989). [c] Vorherr et al. (1993). [d] Mortishire-Smith et al. (1994). [e] Terzi et al. (1992). [f] The numbers in parentheses are the corresponding numbers of residues. [g] N/R = not reported.

equal extinction coefficients for all components of the amide I′ band (Krimm & Abe, 1972; Krimm & Bandekar, 1986) and by summing all β-components (Byler & Susi, 1986); they are summarized in Table 2 along with corresponding results from previous studies.

To exclude the possibility that the secondary structure of PLB in DMPC was a result of the particular phase of DMPC, spectra were recorded for PLB_{26-52} and PLB reconstituted in supported membranes of POPC, which is in the liquid-crystalline phase at room temperature. The results of the amide I′ band decompositions of these spectra are included in Tables 1 and 2. Comparison of the data obtained for DMPC and POPC shows that the overall secondary structure of PLB is very similar in these two lipids. The largest difference is an increase in the number of helical residues in PLB_{26-52} from 20 (DMPC) to 22 (POPC). We believe this difference is close to the resolution of the present method and may not be statistically significant.

PLB, reconstituted in substrate-supported DMPC bilayers, was phosphorylated by incubation of the sample in the presence of the catalytic subunit of PKA and ATP. To verify the incorporation of the phosphate group in PLB, the spectra were compared in the region of the phosphate stretching vibration (Figure 6). After phosphorylation, a new peak appeared around 1200 cm^{-1} which is clearly seen in the difference spectrum in the inset of Figure 6. This new peak at 1200 cm^{-1} most likely results from the antisymmetric stretching vibration of the phosphodioxy group of phosphorylated PLB. This wavenumber is similar to that observed for the antisymmetric stretching vibrations of the phosphodioxy groups of dimethyl phosphates which occur at 1211–1217 cm^{-1} (Guan et al., 1994). The small discrepancy may be due to the ester linkage to Ser-16 of PLB instead of to the methanol group or by hydration of the phosphate group by D_2O. The peak around 1230 cm^{-1} is assigned to the antisymmetric stretching vibration of the phosphate group of the phospholipids (Mendelsohn & Mantsch, 1986; Petersheim et al., 1989). This spectroscopic evidence for PLB phosphorylation *in situ* strongly supports our conclusion that the changes in the secondary structure of PLB are a direct result of the phosphorylation of the protein by PKA.

Next, we determined the orientations of the α-helices of PLB_{26-52}, PLB, and P-PLB in lipid bilayers. The ratios of

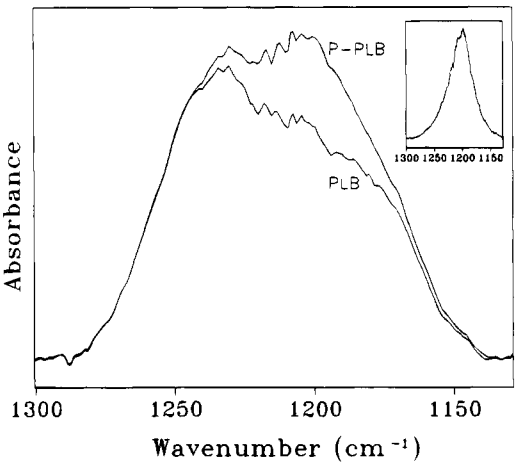

FIGURE 6: Absorbance spectra of PLB and P-PLB, reconstituted in substrate-supported DMPC bilayers, in the phosphate stretching region. The spectrum shown in the inset is the difference between the two spectra.

the areas of the α-helical components of the amide I′ bands of PLB_{26-52} at parallel and perpendicular polarizations were used to find the ATR dichroic ratio of the transmembrane α-helix in DMPC membranes: $R^{ATR} = 3.06 \pm 0.20$. The corresponding order parameter was then calculated through eq 4 as $S = 0.86 \pm 0.09$, using $\alpha = 39°$, $\gamma = 45°$, $n_1 = 4$, $n_2 = 1.43$, and $n_3 = 1.33$ (Tamm & Tatulian, 1993). This implies that the orientation of the transmembrane helix of PLB is almost perpendicular to the membrane plane; the average angle between its long axis and the membrane normal is 18 ± 6°. The ATR dichroic ratios of PLB and P-PLB were $R_T^{ATR} = 2.28 \pm 0.11$ and 2.57 ± 0.16, respectively. These values of R_T^{ATR}, combined with $S_1 = 0.86 \pm 0.09$, were used in eq 6 to find the order parameter of the cytoplasmic helix of PLB and P-PLB; they were $S_2 = -0.15 \pm 0.30$ and 0.09 ± 0.41, which are consistent either with fixed angles between the cytoplasmic helix and the membrane normal of $\theta = 61 \pm 13°$ and $51 \pm 19°$, respectively, or with the average of a nearly random orientational distribution of the cytoplasmic helix.

The order parameter of the lipid acyl chains was evaluated to determine whether the order of the phospholipid bilayer was perturbed by the incorporated peptides. Polarized ATR-FTIR spectra of the DMPC bilayer with reconstituted PLB

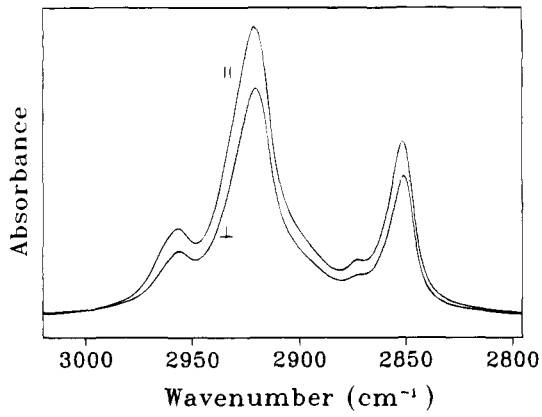

FIGURE 7: Absorbance spectra of DMPC bilayers with incorporated PLB in the region of CH_2 stretching vibrations at parallel and perpendicular polarizations of the IR beam, as indicated.

in the region of the CH_2 stretching vibrations are presented in Figure 7. The ratio of the peak absorbances for the antisymmetric (2920.6 cm^{-1}) and symmetric (2851.0 cm^{-1}) methylene stretching vibrations at parallel and perpendicular polarizations yielded the ATR dichroic ratio for the lipid acyl chains, namely, $R^{ATR} = 1.25 \pm 0.02$. Then eq 4 was used (with $\alpha = 90°$) to evaluate the order parameter of the acyl chains: $S_L = 0.45 \pm 0.02$. These values of R^{ATR} and S_L are in good agreement with the ATR-FTIR data of Hübner and Mantsch (1991), who measured R^{ATR} of DMPC multibilayers as ~1.1 below and ~1.3 above the lipid phase transition temperature. The data indicate that in our experiments the phospholipid bilayers were well ordered and probably contained both gel and liquid-crystalline phases. The latter is confirmed by the position of the peak resulting from the CH_2 symmetric stretching vibration at 2851.0 cm^{-1} (Figure 7), which corresponds to the frequency found at the midpoint of the thermal phase transition of DMPC or dipalmitoylphosphatidylcholine bilayers (Cameron et al., 1980; Bouchard & Auger, 1993). Measurements of the dichroic ratio of the acyl chains of POPC/PLB bilayers yielded a very low value of $S_L = 0.11 \pm 0.01$, which precluded determinations of the orientation of PLB in this lipid.

DISCUSSION

We have determined the secondary structures of PLB, phosphorylated PLB, and the transmembrane peptide PLB_{26-52} in lipid bilayers using ATR-FTIR spectroscopy. The secondary structures of PLB and PLB peptides were previously measured in detergent micelles or organic/aqueous solvents using CD and NMR. The various results are summarized in Table 2. Generally, there is good agreement between the different studies. We find 33−35 α-helical residues in PLB, about 20 of which can be attributed to the transmembrane peptide. Similar results were previously reported for these two polypeptides in SDS micelles (Simmerman et al., 1989). According to our results, the cytoplasmic peptide contains ~13 residues in α-helical conformation, which is in reasonable agreement with CD and NMR data on the cytoplasmic fragment in 30% TFE/70% H_2O (Mortishire-Smith et al., 1994). We also find ~6 residues in β-strand and ~13 residues in random coil conformation for PLB reconstituted in DMPC bilayers.

Apparently, the amide protons of the α-helices of PLB were not readily exchanged for deuterons after several hours of exposure to D_2O at room temperature. This is evident from the positions of the peaks of the whole amide I′ bands and of their α-helical components at 1655−1657 cm^{-1} (Figures 3−5). The shoulder of the amide I′ bands of PLB and P-PLB at ~1640 cm^{-1} indicates that the amide protons of the random structure are extensively exchanged for deuterons. This is consistent with the notion that hydrogens exchange very slowly in stable secondary structures, but much more rapidly in random structures of proteins as detected, for example, in cytochrome *c* (Heimburg & Marsh, 1993). Similar to the present results with PLB, the amide protons of a model transmembrane α-helix did not readily exchange in D_2O at room temperature (Zhang et al., 1992).

The major effect of phosphorylation of PLB by PKA is an increase of random structure by ~5 residues at the expense of the cytoplasmic helix, which is generally consistent with previous reports. In particular, the magnitude of this change is in good agreement with the NMR results of Mortishire-Smith et al. (1994) on the cytoplasmic peptide PLB_{1-25}, and the absolute number of α-helical residues in the cytoplasmic domain after phosphorylation (eight) agrees with the CD data of Terzi et al. (1992). However, some studies have reported smaller or larger numbers of residues changing from α-helix to random coil upon phosphorylation. For instance, Simmerman et al. (1989) found by CD only 1−2 residues to be involved in the phosphorylation-induced conformational change of full-length PLB in SDS micelles, whereas Mortishire-Smith et al. (1994) reported about nine residues to be involved in this structural change based on their CD experiments on PLB_{1-25}.

Determination of the absolute number of residues involved in the conformational change upon phosphorylation depends on the stoichiometry of phosphorylation. For two reasons, we think that most PLB molecules were incorporated into the supported membranes with a right-side-out, PKA-accessible orientation, i.e., with the amino terminus facing the bulk aqueous compartment: (a) although there is a thin gap between the membrane and its solid support, it is probably too small to accomodate the cytoplasmic domain, and (b) influenza hemagglutinin that was reconstituted in supported membranes by the same method was recently shown to be oriented at least 90% right-side-out (Hinterdorfer et al., 1994). Nevertheless, it is worth noting that if only a fraction of all PLB molecules were phosphorylated, the resulting conformational change would involve a larger number of residues.

Some of the quantitative differences between the data of different authors, shown in Table 2, may be due to the different experimental methods and conditions used. Our results are the only ones that were obtained with PLB reconstituted in lipid bilayers, and this is the first FTIR spectroscopic study on the structure of PLB. Also, the structure of the cytoplasmic domain may be influenced by the presence of the transmembrane domain in the intact molecule. Nevertheless, given these large differences in experimental approach, the general agreement between the various data of Table 2 is quite remarkable.

Comparison of the structure of PLB and its transmembrane peptide PLB_{26-52} in DMPC and POPC summarized in Tables 1 and 2 shows that the α-helical fraction of PLB_{26-52} in POPC is increased by 9% (~2 residues) as compared to that in DMPC. Also, the component at ~1674−1677 cm^{-1} is slightly increased at the expense of the component at

~1620−1630 cm^{-1}. Although these differences may reflect some minor change in the structure of the peptide PLB_{26-52} in DMPC and POPC (PLB_{26-52} in POPC could have a turn-like structure instead of β-structure at its amino terminus, represented by the component at 1674−1677 cm^{-1}), these changes (1−2 residues) are close to the resolution limit of the present method and may not be significant. In any case, we still conclude that this transmembrane peptide is predominantly α-helical.

In order to find the most likely positions for the cytoplasmic α-helix and antiparallel β-sheet, the cytoplasmic sequence of PLB was analyzed by the Chou−Fasman secondary structure prediction program (Chou & Fasman, 1974). The results are included in Figure 1. An α-helical conformation was predicted for the 12 residues between Arg-9 and Met-20. This is in good agreement with a 13-residue cytoplasmic α-helix that we found experimentally. Combining our experimental results with these secondary structure predictions, we propose a working model for the structure of PLB (Figure 8). Since Pro-21 is a helix breaker (Chou & Fasman, 1974), it is likely that the cytoplasmic helix extends from Thr-8 to Met-20. The Chou−Fasman program predicts two stretches of β-structure, namely, Val-4 to Thr-8 and Gln-22 to Phe-32, and our data indicate 6−7 residues of antiparallel β-sheet. Intermolecular antiparallel strand-pairing between different PLB molecules seems unlikely for steric reasons if one takes into account the result that PLB forms pentamers via interactions of its hydrophobic helices (Simmerman et al., 1994; Arkin et al., 1994). This leaves us with two possibilities for intramolecular strand-pairing, namely, an association of the two predicted regions of β-structure or a short double-stranded antiparallel β-sheet between the two α-helices. The first possibility is rejected because the two strands forming the pair are separated by the 13-residue cytoplasmic helix. Therefore, the antiparallel β-sheet most likely extends from Gln-22 to Phe-32. Following the Chou−Fasman rules, residues Gln-22 to Gln-26 and Leu-31 to Phe-32 would constitute the two strands of the β-sheet, and the best candidates for the turn are Asn-27, Leu-28, Gln-29, and Asn-30, because Asn has both α-helix- and β-strand-breaking capacity and high predilection for turns (Chou & Fasman, 1974). However, in this case three of the five residues of the longer strand would not have partners for hydrogen bonding. Therefore we suggest a symmetric antiparallel β-sheet, as shown in Figures 1 and 8, with a turn including the residues Gln-26, Asn-27, Leu-28, and Gln-29. This does not contradict Chou−Fasman, because Gln is rather indifferent towards any secondary structure. We cannot discriminate between different types of turn because turns give rise to vibrations with many characteristic frequencies, including 1653−1656 cm^{-1} and 1671−1677 cm^{-1} (Krimm & Bandekar, 1986), and the expected turn component of the amide I′ band may be masked by the α-helical or the high frequency β-strand modes. Given these assignments, the amino-terminal residues Met-1 to Leu-7 are likely to adopt a random structure.

The order parameters of the two α-helices were determined individually by measuring the dichroic ratios of the α-helical component bands. The order parameter of the transmembrane α-helix was 0.86 ± 0.09, which is close to the theoretical limit of 1.0 for a perfect alignment of the helix parallel to the membrane normal. If all helices were aligned at the same rigid angle with respect to the membrane normal,

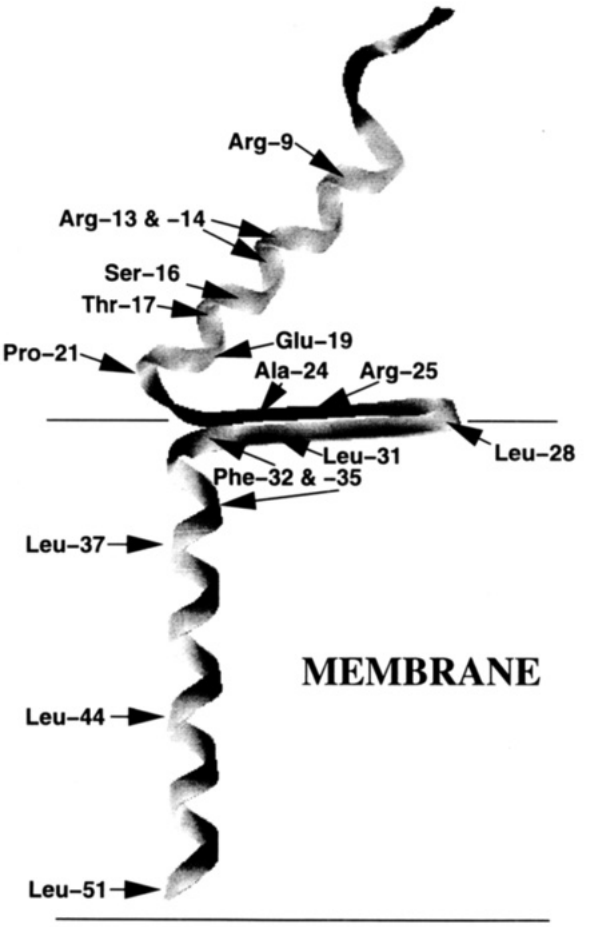

FIGURE 8: Model of the structure of phospholamban in a lipid bilayer based on FTIR results and Chou−Fasman predictions for secondary structure. The cytoplasmic α-helix includes residues 8−20 and is interrupted by Pro-21. Residues 22−32 form an antiparallel β-sheet, and the residues 33−52 constitute the transmembrane α-helix. The residues 1−7 form a random coil at the amino terminus of the molecule (see text for assignments). The transmembrane helix is shown perpendicular to the membrane plane. The angle between the cytoplasmic helix and the membrane normal could vary in a wide range or may be fixed at 50−60° (see text). The β-sheet is proposed to be located at the membrane−water interface because of its amphiphilic character. The azimuthal orientation of the cytoplasmic helix and the β-sheet relative to one another and around the transmembrane helix is not known. However, to allow for pentamer formation, they are both constructed in a direction approximately opposite to leucines 37, 44, and 51 which are essential for subunit interaction (Simmerman et al., 1994; Arkin et al., 1994).

this angle would be 18°. The order parameter of the cytoplasmic α-helix was −0.15 ± 0.30 before and 0.09 ± 0.41 after phosphorylation. The large standard deviations of the order parameters of the cytoplasmic helix are the result of error propagation from two different measurements, namely, S_1 and R_T^{ATR} (see Theory). At the two extremes, these order parameters could be interpreted as fixed angles between the helical axis and the membrane normal $\theta = 61 \pm 13°$ and $51 \pm 19°$, respectively, or as approximately random orientational distributions. Despite this ambiguity, our results exclude the possibility that the cytoplasmic helix is oriented either parallel or perpendicular to the membrane.

Given the structural model of PLB presented in Figure 8, it is still difficult to predict how PLB may regulate Ca^{2+}-ATPase. The orientation of the cytoplasmic helix, and perhaps even the whole structure of PLB, may be different when it makes contact with the ATPase in cardiac SR. The

stalk region of the ATPase is highly anionic, and electrostatic attraction between this region and the cationic face of the cytoplasmic peptide of PLB has been proposed (MacLennan et al., 1985; Tada & Kadoma, 1989; Vorherr et al., 1992). Phosphorylation of PLB is likely to reduce or even prevent this electrostatic attraction. Our data indicate that the average orientation of the cytoplasmic helix of PLB may become a little more vertical upon phosphorylation. However, the major effect of phosphorylation is a partial unwinding of the cytoplasmic helix. It is possible that the angle between the cytoplasmic helix and the β-sheet is stabilized by ion pair formation between Glu-19 and Arg-25. If this is the case, phosphorylation of Ser-16 may lead to an unwinding of the last turn of the cytoplasmic helix to replace Glu-19 with phosphoserine in the ion pair with Arg-25. This rotation would turn arginines 9, 13, and 14 to the opposite side of the helix which could possibly prevent the interaction of this cationic charge cluster with the negatively charged stalk sector of the Ca^{2+}-ATPase. Of course, structural studies on PLB interacting with the Ca^{2+}-ATPase are required to answer these questions. Nevertheless, the results of this work provide a structural basis for considering the conformational changes that may take place when PLB binds to the ATPase.

REFERENCES

Arkin, I. T., Adams, P. D., MacKenzie, K. R., Lemmon, M. A., Brünger, A. T., & Engelman, D. M. (1994) *EMBO J. 13*, 4757−4764.

Arkin, S., Moczydlowski, E. G., Aimoto, S., Smith, S. O., & Engelman, D. M. (1993) *Biophys. J. 64*, A207.

Arrondo, J. L. R., Muga, A., Castresana, J., & Goñi, F. M. (1993) *Prog. Biophys. Mol. Biol. 59*, 23−56.

Bouchard, M., & Auger, M. (1993) *Biophys. J. 65*, 2484−2492.

Briggs, F. N., Lee, K. F., Wechsler, A. W., & Jones, L. R. (1992) *J. Biol. Chem. 267*, 26056−26061.

Byler, D. M., & Susi, H. (1986) *Biopolymers 25*, 469−487.

Cala, S. E., O'Brian, J. J., & Jones, L. R. (1993) *Biophys. J. 64*, A375.

Cameron, D. G., Casal, H. L., & Mantsch, H. H. (1980) *Biochemistry 19*, 3665−3672.

Cantilina, T., Sagara, Y., Inesi, G., & Jones, L. R. (1993) *J. Biol. Chem. 268*, 17018−17025.

Chiesi, M., & Schwaller, R. (1989) *FEBS Lett. 244*, 241−244.

Chou, P. Y., & Fasman, G. D. (1974) *Biochemistry 13*, 222−245.

Frey, S., & Tamm, L. K. (1991) *Biophys. J. 60*, 922−930.

Fringeli, U. P. (1992) *Chimia 46*, 200−214.

Fujii, J., Kadoma, M., Tada, M., Toda, H., & Sakiyama, F. (1986) *Biochem. Biophys. Res. Commun. 138*, 1044−1050.

Fujii, J., Ueno, A., Kitano, K., Kadoma, M., & Tada, M. (1987) *J. Clin. Invest. 79*, 301−304.

Fujii, J., Lytton, J., Tada, M., & MacLennan, D. H. (1988) *FEBS Lett. 227*, 51−55.

Guan, Y., Wurrey, C. J., & Thomas, G. J., Jr. (1994) *Biophys. J. 66*, 225−235.

Harrick, N. J. (1979) in *Internal Reflection Spectroscopy*, Harrick Scientific Corp., Ossining, NY.

Heimburg, T., & Marsh, D. (1993) *Biophys. J. 65*, 2408−2417.

Hinterdorfer, P., Baber, G., & Tamm, L. K. (1994) *J. Biol. Chem. 269*, 20360−20368.

Hübner, W., & Mantsch, H. H. (1991) *Biophys. J. 59*, 1261−1272.

James, P., Inui, M., Tada, M., Chiesi, M., & Carafoli, E. (1989) *Nature 342*, 90−92.

Jones, L. R., Simmerman, H. K. B., Wilson, W. W., Gurd, F. R. N., & Wegener, A. D. (1985) *J. Biol. Chem. 260*, 7721−7730.

Jorgensen, A. O., & Jones, L. R. (1986) *J. Biol. Chem. 261*, 3775−3781.

Kovacs, R. J., Nelson, M. T., Simmerman, H. K. B., & Jones, L. R. (1988) *J. Biol. Chem. 263*, 18364−18368.

Krimm, S., & Abe, Y. (1972) *Proc. Natl. Acad. Sci. U.S.A. 69*, 2788−2792.

Krimm, S., & Bandekar, J. (1986) *Adv. Protein Chem. 38*, 181−364.

Laemmli, U. K. (1970) *Nature 227*, 680−685.

Le Peuch, C. J., Haiech, J., & Demaille J. D. (1979) *Biochemistry 18*, 5150−5157.

Lindemann, J. P., Jones, L. R., Hathaway, D. R., Henry, B. G., & Watanabe, A. M. (1983) *J. Biol. Chem. 258*, 464−471.

MacLennan, D. H., Brandl, C. J., Korczak, B., & Green, N. M. (1985) *Nature 316*, 696−700.

Mendelsohn, R., & Mantsch, H. H. (1986) in *Progress in Protein−Lipid Interaction* (Watts, A., & De Pont, J. J. H. M., Eds.) Vol. 2, pp 103−146, Elsevier, Amsterdam.

Miyazawa, T. (1960) *J. Chem. Phys. 32*, 1647−1652.

Morris, G. L., Cheng, H., Colyer, J., & Wang, J. H. (1991) *J. Biol. Chem. 266*, 11270−11275.

Mortishire-Smith, R., Pitzenberger, S., Gorsky, V. M., Burke, C., Mach, H., Middaugh, C. R., & Johnson, R. G., Jr. (1994) *Biophys. J. 66*, A40.

Petersheim, M., Halladay, H. N., & Blodnieks, J. (1989) *Biophys. J. 56*, 551−557.

Reddy, L. G., Jones, L. R., Cala, S. E., O'Brian, J. J., Tatulian, S. A., & Stokes, D. L. (1995) *J. Biol. Chem.* (in press).

Schaffner, W., & Weissman, C. (1973) *Anal. Biochem. 56*, 502−514.

Sham, J. S. K., Jones, L. R., & Morad, M. (1991) *Am. J. Physiol. 261*, H1344−H1349.

Simmerman, H. K. B., Collins, J. H., Theibert, J. L., Wegener, A. D., & Jones, L. R. (1986) *J. Biol. Chem. 261*, 13333−13341.

Simmerman, H. K. B., Lovelace, D. E., & Jones, L. R. (1989) *Biochim. Biophys. Acta 997*, 322−329.

Simmerman, H. K. B., Kobayashi, Y. M., Strifler, B., & Jones, L. R. (1994) *Biophys. J. 66*, A178.

Surewicz, W. K., Mantsch, H. H., & Chapman, D. (1993) *Biochemistry 32*, 389−394.

Szimanska, G., Kim, H. W., Cuppoletti, J., & Kranias, E. G. (1991) *Membr. Biochem. 9*, 191−202.

Tada, M., & Kadoma, M. (1989) *BioEssays 10*, 157−163.

Tamm, L. K., & Tatulian, S. A. (1993) *Biochemistry 32*, 7720−7726.

Terzi, E., Poteur, L., & Trifilieff, E. (1992) *FEBS Lett. 309*, 413−416.

Toyofuku, T., Kurzydlowski, K., Tada, M., & MacLennan, D. H. (1993) *J. Biol. Chem. 268*, 2809−2815.

Toyofuku, T., Tada, M., & MacLennan, D. H. (1994) *Biophys. J. 66*, A121.

Vorherr, T., Chiesi, M., Schwaller, R., & Carafoli, E. (1992) *Biochemistry 31*, 371−376.

Vorherr, T., Wrzosek, A., Chiesi, M., & Carafoli, E. (1993) *Protein Sci. 2*, 339−347.

Voss, J., Jones, L. R., & Thomas, D. D. (1994) *Biophys. J. 67*, 190−196.

Wegener, A. D., & Jones, L. R. (1984) *J. Biol. Chem. 259*, 1834−1841.

Wegener, A. D., Simmerman, H. K. B., Liepnieks, J., & Jones, L. R. (1986) *J. Biol. Chem. 261*, 5154−5159.

Zhang, Y.-P., Lewis, R. N. A. H., Hodges, R. S., & McElhaney, R. N. (1992) *Biochemistry 31*, 11572−11578.

BI942071E